

## Energy bands and acceptor binding energies of GaN

Jian-Bai Xia and K. W. Cheah

*Department of Physics, Hong Kong Baptist University, Kowloon Tong, Hong Kong, China*

Xiao-Liang Wang, Dian-Zhao Sun, and Mei-Ying Kong

*Semiconductor Materials Center, Institute of Semiconductors, Chinese Academy of Sciences, Beijing 100083, China*

(Received 7 July 1998)

The energy bands of zinc-blende and wurtzite GaN are calculated with the empirical pseudopotential method, and the pseudopotential parameters for Ga and N atoms are given. The calculated energy bands are in agreement with those obtained by the *ab initio* method. The effective-mass theory for the semiconductors of wurtzite structure is established, and the effective-mass parameters of GaN for both structures are given. The binding energies of acceptor states are calculated by solving strictly the effective-mass equations. The binding energies of donor and acceptor are 24 and 142 meV for the zinc-blende structure, 20 and 131, and 97 meV for the wurtzite structure, respectively, which are consistent with recent experimental results. It is proposed that there are two kinds of acceptor in wurtzite GaN. One kind is the general acceptor such as C, which substitutes N, which satisfies the effective-mass theory. The other kind of acceptor includes Mg, Zn, Cd, etc., the binding energy of these acceptors is deviated from that given by the effective-mass theory. In this report, wurtzite GaN is grown by the molecular-beam epitaxy method, and the photoluminescence spectra were measured. Three main peaks are assigned to the donor-acceptor transitions from two kinds of acceptors. Some of the transitions were identified as coming from the cubic phase of GaN, which appears randomly within the predominantly hexagonal material. [S0163-1829(99)15915-0]

### I. INTRODUCTION

In the past several years GaN of either hexagonal or cubic structures has created increasing interest due to the wide application in blue light emitting diodes and lasers. Many optical measurement results have been published,<sup>1-5</sup> and various photoluminescence (PL) peaks have been identified, for example, free exciton, donor bound exciton, acceptor bound exciton, and donor-acceptor transition, etc. For the cubic GaN, which has a crystal structure and energy band similar to those of general III-V compound semiconductors with zinc-blende structure, the binding energies of exciton, donor, and acceptor estimated from the optical experiments are all in the reasonable range. On the other hand, for the wurtzite GaN the binding energy of acceptor obtained from the optical data is not definite. Previous experimental works<sup>2,3</sup> assigned the 3.26-eV PL peak as the donor-acceptor (DA) transition, so the binding energy of the acceptor state will be about 200 meV. Orton<sup>6</sup> replaced the static dielectric constant by the high-frequency dielectric constant in order to explain the large binding energy of acceptor. Pödör<sup>7</sup> established a correlation between the acceptor ionization energies and the chemical nature of the acceptor atoms by considering the electronegativity differences between the acceptor atoms and the host atom they substitute. Based on this, the effective-mass acceptor ionization energy in GaN is estimated to be  $85 \pm 8$  meV. In a recent optical experiment<sup>5</sup> Ren *et al.* observed a new line at approximately 3.40 eV, which is accompanied by complex fine structure, and interpreted it as due to a DA transition. Assuming a donor binding energy of 30 meV, they derived an acceptor binding energy of approximately 80 meV. They also assigned the 3.265-eV peak, which often assigned as a DA transition, as a  $D^0X$  transition

from cubic GaN inclusions occurring randomly within the predominantly hexagonal material. McGill *et al.*<sup>8</sup> obtained the polaron mass  $0.75m_0$  instead of the band effective mass  $0.5-0.6m_0$ , leading to a predicted thermal binding energy in the effective-mass limit of  $\sim 100-125$  meV. There have been many theoretical calculations of GaN energy bands, especially the wurtzite structure. These theories based on the empirical pseudopotential method<sup>9-12</sup> and the first-principle pseudopotential or other methods,<sup>13-17</sup> where Suzuki, Uenoyama, and Yanase<sup>17</sup> derived the effective-mass parameters of conduction and valence bands.

In this paper we first calculate the energy bands of GaN of both structures by the empirical pseudopotential method. Based on the calculated energy bands of GaN, we derive the effective-mass parameters for both structures, and calculate the binding energies of donors, acceptors and excitons using the effective-mass theory. To correlate our theoretical calculations we grew two GaN thin films on sapphire substrate and measured their photoluminescence characteristic. Section II is the empirical pseudopotential calculations of energy bands for zinc-blende and wurtzite GaN, and Sec. III gives the calculation of the binding energies of acceptors and excitons by the effective-mass theory for the degenerate bands. Section IV is the experimental details and results, and Sec. V is the summary.

### II. EMPIRICAL PSEUDOPOTENTIAL CALCULATION OF GaN ENERGY BANDS

First we fit the form factors of the atomic pseudopotential of Ga and N with the Cohen's formula<sup>18</sup>

$$V(G) = \frac{v_1(G^2 - v_2)}{e^{v_3(G^2 - v_4)} + 1}, \quad (1)$$

TABLE I. Fitting parameters of Ga and N atomic pseudopotentials.

	$\nu_1$	$\nu_2$	$\nu_3$	$\nu_4$
Ga	0.176 825	1.833 41	1.600 00	1.819 52
N	0.326 847	4.282 26	0.700 00	2.605 61

where  $\nu_1$ ,  $\nu_2$ ,  $\nu_3$ , and  $\nu_4$  are empirical parameters determined by the experimental energy values at some special points in the Brillouin zone or more precise energy band calculation results. Table I gives the fitted  $\nu_1$ - $\nu_4$  values for the Ga and N atomic pseudopotentials, where the unit of  $G$  is a.u.<sup>-1</sup>, the unit of  $V(G)$  is Ry, which is normalized to the atomic volume in the zinc-blend GaN  $(4.5 \text{ \AA})^3/8$ . The cutoff wave vector in the calculating energy band is taken as 2.8 a.u.<sup>-1</sup>. Using the same atomic pseudopotentials we calculated the energy bands of zinc-blende and wurtzite GaN. The lattice constants for the two GaN structures are taken as  $a = 4.50 \text{ \AA}$  (cubic), and  $a = 3.189$ ,  $c = 5.185 \text{ \AA}$  (hexagonal), and the calculated energy gaps are 3.389 and 3.500 eV, respectively. The valence bands near the valence-band top for the wurtzite structure are shown in Fig. 1, where the  $\Gamma_6$  energy level is higher than the  $\Gamma_1$  energy level by 0.02 eV. The calculated energy bands for the wurtzite structure are in agreement with those calculated by the first-principles pseudopotential method,<sup>16</sup> especially the energy gap and the

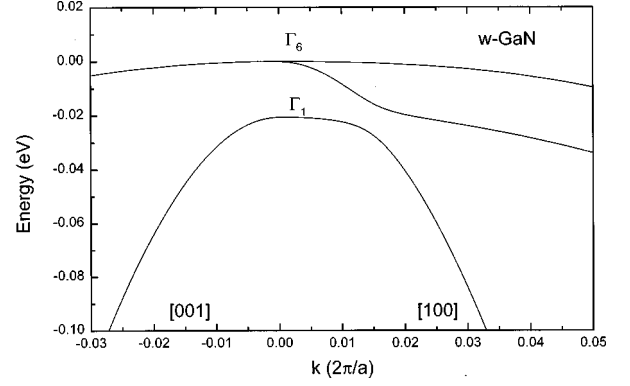


FIG. 1. Valence bands of wurtzite GaN near the  $\Gamma$  point.

crystal-field splitting energy. In this paper the symmetry symbols are according to Slater<sup>19</sup> for the  $C_{6v}$  (Ref. 4) space group and its  $k$  group.

### III. EFFECTIVE-MASS THEORY

The effective-mass theory of acceptor states for the semiconductors of diamond or zinc-blende structures has been derived earlier.<sup>20</sup> Because the spin-orbital splitting of the valence band of GaN is very small<sup>21</sup> (10 meV), so in the following we use the effective-mass equation in the zero spin-orbital splitting limits. For the zinc-blende GaN the effective-mass Hamiltonian of the acceptor state is

$$H_a = \frac{1}{2m_0} \begin{vmatrix} Lp_x^2 + M(p_y^2 + p_z^2) & Np_xp_y & Np_xp_z \\ Np_xp_y & Lp_y^2 + M(p_x^2 + p_z^2) & Np_y p_z \\ Np_xp_z & Np_y p_z & Lp_z^2 + M(p_x^2 + p_y^2) \end{vmatrix} - \frac{e^2}{\epsilon_0 r}, \quad (2)$$

where  $L, M, N$  are Luttinger effective-mass parameters,<sup>20</sup> and  $\epsilon_0$  is the static dielectric constant. The Luttinger parameters  $L, M, N$  of the zinc-blende GaN have been determined from the highest threefold degenerate valence bands near the  $\Gamma$  point at  $k = 0.028 (2\pi/a)$ , which together with the electron effective mass  $m_e^*$  are listed in Table II.

Baldereschi and Lipari<sup>22</sup> have proved that the Hamiltonian (2) can be written as the following form in the spherical symmetric approximation:

$$H_{sph} = \frac{\gamma_1}{2m_0} \left[ p^2 - \frac{\mu}{3} P^{(2)} \cdot I^{(2)} \right] - \frac{e^2}{\epsilon_0 r}, \quad (3)$$

where  $P^{(2)}$  and  $I^{(2)}$  are the second-rank ( $l=2$ ) irreducible tensor of the momentum operator and the angular momentum operator  $I=1$ ;  $\gamma_1, \mu$  are also the Luttinger effective-mass parameters, which are related to  $L, M, N$  by

$$\gamma_1 = \frac{L+2M}{3}, \quad \mu = \frac{2(l-M)+3N}{5(L+2M)}. \quad (4)$$

The nonspherical cubic term in the Hamiltonian has been neglected. As shown in Ref. 22, the effective-mass equation has the form of a  $2 \times 2$  matrix, which couples the  $L$  state and  $L+2$  states, where  $L$  is the angular momentum quantum number. The acceptor state has the total angular momentum

TABLE II. Effective-mass parameters of zinc-blende and wurtzite GaN.

	$m_e^*$	$L$	$M$	$N$	$\gamma_1$	$\mu$			
Zinc blende	0.1388	6.09	1.045	6.95	2.7267	0.7565			
	$m_e^*$	$L$	$M$	$N$	$R$	$S$	$T$	$Q$	$A$
Wurtzite	0.1441( $x$ )	6.3055	0.1956	0.3813	6.1227	0.4355	7.3308	4.0200	0.6751
	0.1395( $z$ )								

TABLE III. Binding energies of donors and acceptors of GaN (in units of MeV, related to the valence-band top).

	$n$	1	2	3	4	5
Zinc blende	Donor $s$	23.8	6.0			
	$S_1$	142.2	42.7	21.4	12.9	8.7
	$P_0$		6.3			
	$P_1$		64.7	28.7	16.2	10.3
	$P_2$		40.2	19.6	11.9	8.1
Wurtzite	Donor $s$	20.2	5.0			
	$\Gamma_1 S$	97.5	42.3	27.0	21.9	13.9
		78.0	9.6	-4.8	-10.8	-14.4
	$\Gamma_6 S$	130.7	41.6	34.3	21.9	14.5
		130.2	41.1	21.7	10.2	5.1

$J=L+I$  with  $I=1$ , for example,  $S_1, P_0, P_1 < P_2, D_1, \dots$  states, where the subscript represents the total angular momentum quantum number. Using the nonorthogonal Gaussian functions as basic functions to expand the wave function (Ref. 22), we solve the effective-mass equation and obtain the binding energies of acceptors listed in Table III, where  $n$  is the ‘‘main’’ quantum number of the impurity states. From Table III we see that the ground acceptor state ( $n=1$ ) in the zinc-blende GaN has large binding energy, 142 meV, the hole effective mass derived from the simple hydrogenlike

model is  $0.83m_0$  ( $\epsilon_0=8.9$ ). While the electron effective mass is  $0.14m_0$ , the corresponding binding energy of donor state is 24 meV. In their cathodoluminescence (CL) experiment of cubic GaN, Menniger *et al.*<sup>4</sup> assigned the lines at 3.234 and 3.208 eV tentatively as free to bound transitions involving the neutral donor and acceptor level, respectively. This in turns yield donor and acceptor binding energies of 68 and 94 meV, respectively. The sum of the binding energies of donor and acceptor from our theoretical calculation is 166 meV, which is in good agreement with the experimental results 162 meV. It seems impossible that the electron has the effective mass as large as that of hole, so our theoretical result is more reasonable, and also gives the 3.15-eV peak of ( $D^0, A^0$ ) transition.<sup>4</sup>

In order to derive the effective-mass equation of wurtzite GaN we use the  $\mathbf{k} \cdot \mathbf{p}$  perturbation theory.<sup>20</sup> The valence-band top states belong to the representations  $\Gamma_6$  (twofold degenerate) and  $\Gamma_1$  (onefold degenerate) of the  $k$  group  $C_{6v}$  at the  $\Gamma$  point,<sup>19</sup> which are separated by a crystal-field splitting energy  $E_0$  of approximately 0.02 eV. The component of momentum operator  $p_z$  belongs to the  $\Gamma_1$  representation, and the  $p_x$  and  $p_y$  belong to the  $\Gamma_6$  representation. Through the  $\mathbf{k} \cdot \mathbf{p}$  perturbation operator the states of the valence-band top at the  $\Gamma$  point can interact with other states at the  $\Gamma$  point or each other, then we obtain the effective-mass Hamiltonian as follows:

$$H = -\frac{1}{2m_0} \begin{vmatrix} Lp_x^2 + Mp_y^2 + Np_z^2 & Rp_x p_y & Ap_0 p_x + Qp_x p_z \\ Rp_x p_y & Lp_y^2 + Mp_x^2 + Np_z^2 & Ap_0 p_y + Qp_y p_z \\ Ap_0 p_x + Qp_x p_z & Ap_0 p_y + p_y p_z & S(p_x^2 + p_y^2) + Tp_z^2 + E_0 \end{vmatrix}, \quad (5)$$

where the basic functions are  $X$  like,  $Y$  like ( $\Gamma_6$ ), and  $Z$  like ( $\Gamma_1$ ) functions, respectively, and  $L, M, \dots, S, T$  are all effective-mass parameters. It is noticed that the existence of the linear term of  $p_x$  and  $p_y$  results in the anticrossing of  $\Gamma_6$  and  $\Gamma_1$  energy bands as shown in Fig. 1, where the highest valence band in the [100] and [001] directions near  $2\Gamma$  point are given. The effective-mass Hamiltonian (5) is different from that derived in previous works,<sup>17,24</sup> where they neglected the  $p$ -linear terms. The  $p$ -linear terms are important for the case of small crystal-field splitting energy, because they cannot be replaced by the  $p$ -quadratic terms with the second-order perturbation theory. This  $p(k)$ -linear term has been verified experimentally for the wurtzite CdS,<sup>25</sup> which has the similar crystal-field splitting energy as GaN (27 meV). To make the coefficient  $A$  of the linear term dimensionless we introduce  $p_0 = (2m_0 E_0)^{1/2}$ . The effective-mass parameters are determined by fitting the calculated energy bands at small wave vectors, they are given in Table II. To calculate the binding energy of acceptors, we should solve a set of three coupled equations given by the Hamiltonian (5). The wave function of acceptor state is composed of three components, each component is expanded as a linear combination of Gaussian orbitals with different exponents in the  $x$ ,

$y$ , and  $z$  directions.<sup>23</sup> From Table II we see that for the diagonal terms in the Hamiltonian (5) there is always one direction with large effective-mass parameters, and other two directions with small effective-mass parameters. For example,  $L \gg M$ ,  $N$  and  $T \gg S$  for the first two and the third diagonal terms in the Hamiltonian (5), respectively. Therefore we expand each component of acceptor state wave function by the Gaussian functions with different exponential coefficients in one direction and other two directions.<sup>23</sup> For example, for the  $s$ -like state of the third component we take

$$\psi = \sum_{i,j} C_{ij} \left( \frac{2\alpha_i}{\pi} \right)^{1/4} e^{-\alpha_i z^2} \left( \frac{2\beta_j}{\pi} \right)^{1/2} e^{-\beta_j(x^2 + y^2)}, \quad (6)$$

where the coefficients are the normalization constants. The Gaussian functions of the  $p$ - ( $z$ -) like and  $p$ - ( $x$ -) like states are given in Ref. 23.

For the first and second components, we only need to exchange the corresponding coordinates in Gaussian functions (6). The exponential  $\alpha_i$  and  $\beta_j$  are taken to make the spatial distribution of Gaussian orbitals consistent with the wave function. Generally they are inversely proportional to the corresponding effective-mass parameters.<sup>23</sup> In the following we use an average effective-mass parameter instead

of the effective-mass parameters  $M$  and  $N$ . The matrix elements of Hamiltonian, especially that of Coulomb interaction term, can all be calculated analytically.<sup>23</sup> Because the spacing between the  $\Gamma_6$  and  $\Gamma_1$  energy levels is small (20 meV), there is strong coupling between these two states.

In this way we obtain the binding energies of acceptor  $\Gamma_6S$  and  $\Gamma_1S$  states, shown in Table III, where the binding energies of donor state are also given. The  $\Gamma_6S$  and  $\Gamma_1S$  states are composed mainly of  $S$  states of  $\Gamma_6$  band or  $\Gamma_1$  band, respectively. The second line in Table III gives the binding energies of the acceptor states calculated in the single-band approximation. Comparing the binding energies with and without coupling (second line) we found that the binding energy of the  $\Gamma_6S$  ground state changes slightly after taking into account the interband coupling, but the binding energies of  $\Gamma_1S$  states change significantly. From Table III the binding energies of the ground  $\Gamma_1S$  state are 97.5 and 78.0 meV for with and without inter-band coupling, respectively, so the binding energy of the ground state increases by 19.5 meV by taking into account the inter-band coupling. From the Hamiltonian (5) we see that the  $\Gamma_1S$  state couples mainly with  $\Gamma_6X$  and  $\Gamma_6Y$  states (in our case we neglect the higher-order coupling terms  $Qp_xp_z$  and  $Qp_y p_z$ ), and the coupling is stronger. The  $\Gamma_6S$  states are twofold degenerate, one of them couples with the  $\Gamma_1X$  and  $\Gamma_6XY$  states, and the other couples with the  $\Gamma_1Y$  and  $\Gamma_6XY$  states, respectively. Because the effective Bohr radius is proportional to the related effective-mass parameter, the wave function extends in the direction with larger effective-mass parameter, and shrinks in the direction with smaller effective-mass parameter. From Table II and Hamiltonian (5) we see that the wave function of  $\Gamma_1S$  state extends in the  $z$  direction, while those of two degenerate  $\Gamma_6S$  states extend in the  $x$  and  $y$  directions, respectively. The binding energies for the  $\Gamma_6S$  and  $\Gamma_1S$  ground acceptor states are 131 and 97 meV, respectively ( $\epsilon_0=9.8$ ). The binding energy of the  $\Gamma_1S$  state (97 meV) associated with that of the donor state (20 meV) is in agreement with recent optical experimental result, 80 meV,<sup>5</sup> which was derived by assuming that the binding energy of donor state is 30 meV, and the extrapolated theoretical result was  $85 \pm 8$  meV.<sup>7</sup> The polarization characteristic of PL peaks is easily derived from our theoretical results, it is in the  $z$  direction for the  $D-\Gamma_1S$  transition, and in the  $x,y$  directions for the  $D-\Gamma_6S$  transitions.

The above theory is easily applied to calculate the binding energies of excitons. For the zinc-blende case it only needs to replace the parameters  $\gamma_1$  and  $\mu$  by  $\gamma_1' = \gamma_1 + m_0/m_e^*$  and  $\mu\gamma_1/\gamma_1'$ , respectively in the effective-mass equation of acceptor states Eq. (3).<sup>22</sup> For the wurtzite case it needs to add  $m_0/m_e^*$  to the effective-mass parameters in the momentum terms of the diagonal parts in Hamiltonian (5). The calculated binding energies of excitons for the two cases are listed in Table IV. From Table IV we see that the binding energies of excitons are determined mainly by the effective mass of electron, no matter how complicated the valence band structure is.

The binding energies of acceptor states calculated in this paper has some indefinite factors, first the spacing between the  $\Gamma_6$  and  $\Gamma_1$  bands, 20 meV, is taken from the theoretical result,<sup>16</sup> which has not been verified by the experiment. The

TABLE IV. Binding energies of excitons in GaN (in units of meV).

	$n$	1	2
Zinc blende	$S_1$	18.4	4.4
	$P_0$		3.1
	$P_1$		5.5
	$P_2$		4.5
Wurtzite	$\Gamma_1S$	13.9	3.9
	$\Gamma_6S$	15.9	4.1

amplitude of the spacing between the  $\Gamma_6$  and  $\Gamma_1$  bands will affect the binding energies of the acceptor state. Second the effective-mass parameters are derived from the energy bands calculated by the empirical pseudopotential method. Third we took the average effective-mass parameters of  $M$  and  $N$ . Nevertheless we think the effective-mass theory and the calculation method offer a reasonable result.

#### IV. EXPERIMENTAL DETAILS AND RESULTS

Gas source molecular-beam epitaxy (GSMBE) system used in this work is a modified homemade MBE system with three vacuum chambers. The base pressure in the growth chamber is in the low part of  $10^{-9}$  torr. During growth, a turbomolecular pump was used to keep the pressure in the growth chamber in the range of  $5 \times 10^{-4} \sim 5 \times 10^{-6}$  torr. Ammonia was employed as nitrogen source. High-purity solid gallium was used as gallium source. Sapphire substrates with (0001) orientations were degreased ultrasonically in organic solvents then etched in a hot solution of  $H_2SO_4$  and  $H_3PO_4$  ( $H_2SO_4:H_3PO_4=1:3$ ) mixture for about 20 min. They were then rinsed in deionized water. After spinning dry, the substrates were mounted on molybdenum substrate holders with indium, and loaded into the load lock.

Prior to the growth GaN epilayer, the sapphire substrate was thermally treated in the growth chamber at a temperature as high as 800 °C for about 30 min. Then the ammonia was introduced into the growth chamber to nitridize the sapphire substrate surface at this temperature. Subsequently, the substrate temperature was reduced to about 500 °C and a GaN buffer layer with a thickness of approximately 30 nm was grown. After the low-temperature GaN buffer layer was grown, the substrate temperature was increased to a growth temperature of approximately 750 °C in the presence of ammonia and the gallium was supplied to grow the GaN epitaxial layer. The growth rate was about 0.5  $\mu\text{m/h}$ , and the thickness of the GaN epilayers was approximately 1  $\mu\text{m}$ .

For the PL measurement, the samples were excited by the 325-nm line of a He-Cd laser with a power of 4 mW. PL was taken with a 250-mm double monochromator that has a cooled photomultiplier tube (PMT) as detector. The PMT has a flat response from 300 to 900 nm, and the sample was cooled in a closed-cycle cryostat. The PL spectra of one sample at 10 K are shown in Fig. 2. From Fig. 2 we see two main peaks located at 3.40 and 3.21 eV, respectively. The former has fine structure, while the latter shows no fine structure. The PL is similar to the results of Ref. 5. The multipeak structure for the 3.38–3.40 PL peak is assigned to the transitions from donor state to  $\Gamma_6S$  and  $\Gamma_1S$  acceptor states. We

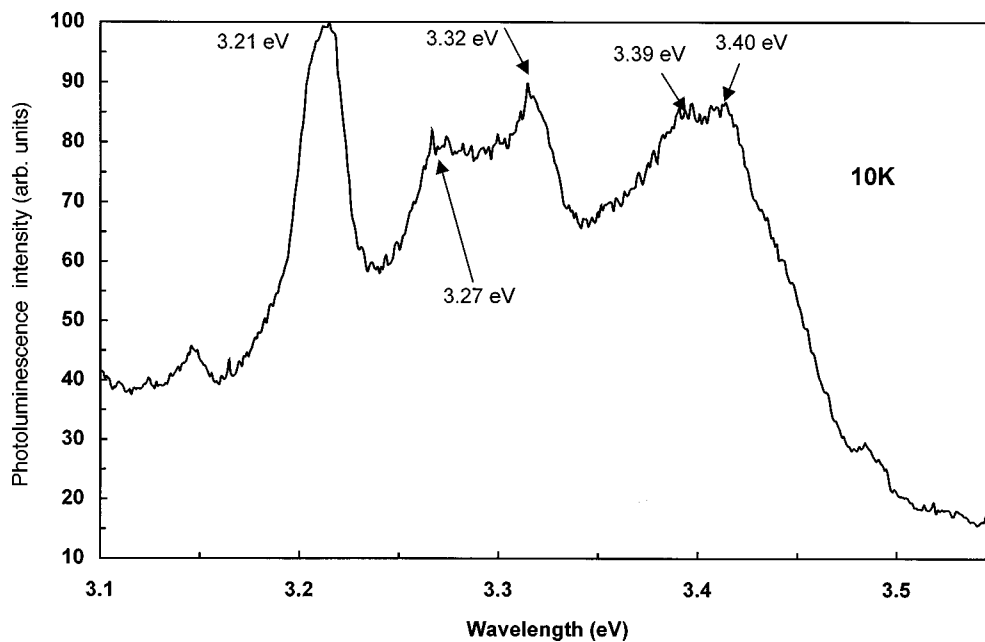


FIG. 2. Photoluminescence spectrum of GaN thin film grown on a sapphire substrate at 10 K.

believe that there are two kinds of acceptor in wurtzite GaN, one is general acceptor such as C, which substitutes N, and the difference of electronegativity between C and N is small. This kind of acceptor satisfies the effective-mass theory. The other kind of acceptor includes Mg, Zn, Cd, etc., the difference of electronegativity between these atoms and substituted atom Ga is large, so the binding energy of these acceptors will be deviated from that given by the effective-mass theory.<sup>7</sup> Therefore we assign the 3.38–3.40 eV peak to the DA transition caused by general acceptor such as C, and the 3.21 eV peak to some transition from cubic GaN inclusions occurring randomly within the predominantly hexagonal material. The 3.25–3.26 eV peak is assigned to the DA transition by the second kind of acceptor such as Mg. The other peaks may be caused by some defects due to lattice mismatch.

## V. SUMMARY

In this paper we calculated the energy bands of zinc-blende and wurtzite GaN with the empirical pseudopotential method, and the pseudopotential parameters for Ga and N atoms are given. The calculated energy bands are in agreement with those obtained by the *ab initio* method. We established the effective-mass theory for the semiconductors of wurtzite structure, and gave the effective-mass parameters of

GaN for both structures. The binding energies of acceptor states are calculated by solving strictly the effective-mass equations. The binding energies of donor and acceptor are 24 and 142 meV for the zinc-blende structure, 20 and 131, 97 meV for the wurtzite structure, respectively, which are consistent with recent experimental results. We proposed that there are two kinds of acceptor in wurtzite GaN. One kind is the general acceptor such as C, which substitutes N, and the difference in electronegativity between C and N is small. This kind of acceptor satisfies the effective-mass theory. Another kind of acceptor includes Mg, Zn, Cd, etc., the difference in electronegativity between these atoms and substituted atom Ga is large, so the binding energy of these acceptors will be deviated from that given by the effective-mass theory. The wurtzite GaN is grown by the GSMBE method, and the PL spectra were measured. Three main peaks are assigned to the DA transitions by the two kinds of acceptors, and some transition from cubic GaN inclusions occurring randomly within the predominantly hexagonal material.

## ACKNOWLEDGMENTS

This project was funded by a RGC grant from Hong Kong, and a National Science Foundation grant of China.

<sup>1</sup>For a review, see S. Strite and H. Morkoc, *J. Vac. Sci. Technol. B* **10**, 1237 (1992).

<sup>2</sup>H. G. Grimmeiss and B. Monemar, *J. Appl. Phys.* **41**, 4054 (1970).

<sup>3</sup>R. Dingle and M. Ilegems, *Solid State Commun.* **9**, 175 (1971).

<sup>4</sup>J. Menniger, U. Jahn, O. Brandt, H. Yang, and K. Ploog, *Phys. Rev. B* **53**, 1881 (1996).

<sup>5</sup>B. G. Ren, J. W. Orton, T. S. Cheng, D. J. Dewsnip, D. E. Lack-

lison, C. T. Foxon, C. H. Malloy, and X. Chen, *MRS Internet J. Nitride Semicond. Res.* **1**, 22 (1997).

<sup>6</sup>J. W. Orton, *Semicond. Sci. Technol.* **10**, 101 (1995).

<sup>7</sup>B. Pödör, *Semicond. Sci. Technol.* **11**, 827 (1996).

<sup>8</sup>S. A. McGill, K. Cao, W. B. Fowler, and G. G. DeLeo, *Phys. Rev. B* **57**, 8951 (1998).

<sup>9</sup>S. Bloom, *J. Phys. Chem. Solids* **32**, 2027 (1971).

<sup>10</sup>J. Bourne and R. L. Jacobs, *J. Phys. C* **5**, 3462 (1972).

- <sup>11</sup>D. Jones and A. H. Lettington, *Solid State Commun.* **11**, 701 (1972).
- <sup>12</sup>S. Bloom, G. Harbeke, E. Meier, and I. B. Ortenburger, *Phys. Status Solidi B* **66**, 161 (1974).
- <sup>13</sup>I. Gorczyca and N. E. Christensen, *Solid State Commun.* **80**, 14 (1991).
- <sup>14</sup>B. J. Min, C. T. Chan, and K. M. Ho, *Phys. Rev. B* **45**, 1159 (1992).
- <sup>15</sup>M. Palummo, C. M. Bertoni, L. Reining, and F. Finocchi, *Physica B* **185**, 404 (1993).
- <sup>16</sup>A. Rubio, J. L. Corkill, M. L. Cohen, E. L. Shirley, and S. G. Louie, *Phys. Rev. B* **48**, 11 810 (1993).
- <sup>17</sup>M. Suzuki, T. Uenoyama, and A. Yanase, *Phys. Rev. B* **52**, 8132 (1995).
- <sup>18</sup>M. Schlütter, J. R. Chelikowsky, S. G. Louie, and M. L. Cohen, *Phys. Rev. B* **12**, 4200 (1975).
- <sup>19</sup>J. C. Slater, *Quantum Theory of Molecules and Solids*, Vol. 2 (McGraw-Hill, New York, 1965).
- <sup>20</sup>J. M. Luttinger, *Phys. Rev.* **102**, 1030 (1956).
- <sup>21</sup>R. Dingle and M. Ilegems, *Solid State Commun.* **9**, 175 (1971).
- <sup>22</sup>A. Baldereschi and N. O. Lipari, *Phys. Rev. B* **8**, 2697 (1973).
- <sup>23</sup>J. B. Xia, *Phys. Rev. B* **39**, 5386 (1989).
- <sup>24</sup>S. L. Chung and C. S. Chang, *Phys. Rev. B* **54**, 2491 (1996).
- <sup>25</sup>E. S. Koteles and G. Winterling, *J. Lumin.* **18/19**, 267 (1979).